

### 3-D Analysis of a 45 Degree Lateral Connection Under Pressure, Mechanical and Thermal Shock Loadings

C. Germain, O. Chedeville

FRAMATOME, Tour Fiat, 1 place de la Coupole, F-92084 Paris-la-Défense, France

#### Abstract

The object of this paper is the stress analysis of 45 degrees safety injection lateral connection. There is one such connection on each cold leg of the primary loop of French 1300 MW power plant. Usually the lack of stress indices (especially for thermal loadings) for such components in design codes (ASME-RCC-M) requires detailed computation. The analysis involves a 3-D finite element method under mechanical and thermal loadings. The special feature of this work is the accuracy of the mesh, which ensures the obtaining of a realistic thermal stress distribution through pipe thickness during fast transients.

#### 1. Introduction

Reactor coolant piping is designed and fabricated to ensure the respect of all safety criteria while supporting all loadings which might be imposed during plant operation. Because of the lack of thermal stress indices for this kind of nozzle, we performe a 3-D finite element analysis on a 45 degrees safety injection nozzle under mechanical and thermal loads. The main function of this connection is to limit the reactor's core temperature when a faulted condition occurs, through the injection of cold water instantly.

The aim of these calculations is to determine the stress state for each point of the structure, at every instant of the analyzed transients. The 3-D model is refined enough to allow thermal stress indices determination during high thermal shocks. In this paper, we describe the thermal and thermal stress analyses.

#### 2. Description of 3-D finite element model

A half symmetric mesh was used and generated automatically by the computer code TITUS (see figure 1). The model consists of 1931 3-D brick elements, each defined by eight nodes (3016 nodes for the whole model). 849 four nodes 2-D elements were added at the inside, outside and end surfaces of the model to determine the surface stresses.

Portions of run and branch pipes are included in the model in order to reduce edge effects due to geometrical discontinuities.

In the circumferential direction, ten identical elements for the branch pipe and the nozzle were taken into account ; see figure 2 for the run pipe section's description.

A parametric analysis on a representative pipe of the lateral connection (thickness equal to the maximum one of the acute corner and length equal to  $5\sqrt{RL}$ ) under thermal step was performed in order to optimize both precision and cost in the special case of thermal shocks. As a result, the mesh was generated with seven elements through wall thickness with

a geometrical increase factor of 1.5 from inside to outside. In order to reduce computer data and computation, the model was broken down into six "super" elements (see figure 3).

### 3. Material properties

This nozzle is made of austeno-ferritic steel SA 351 CF 8 M for which elastic characteristics are  $E:192980$  MPa, and  $\nu: 0.3$ .

### 4. Geometry of the model

The geometrical characteristics of the lateral connection are described on figure 3. Two specific ratios :  $\frac{D}{T}$  (inside diameter to wall thickness) which is : 10.6 for the run pipe and 8.75 for the branch line ;  $\frac{d}{D}$  (branch diameter to run diameter) which is : 0.32.

### 5. Computer codes

Generation of the mesh, thermal analysis and thermoelastic stresses computations were performed with computer code TITUS. Fatigue Analysis according to B 3600, B 3200 and ZE 200 of RCC-M code was performed with the post-processor ROCOCO.

### 6. Thermal loads

Eleven thermal transients covering all power plant operations were selected for heat conduction analysis. Ten transients belong to normal and upset operating conditions :

- (3) - Heatup ; cooldown and shock at the end of cooldown ;
- (2) - Pressure and Temperature monophasic transient ; cooldown with overpressure in monophasic state ;
- (3) - Turbine roll test ; reactor trip ; slow cooling after normal operation ;
- (2) - Inadvertent operation during plant cooldown ; depressurization of the main primary circuit.

We also consider "Loss Of Coolant Accident" transient which belongs to faulted operating conditions.

Outer skin is assumed to be thermally insulated.

Heat exchange coefficient (h) :

For primary transient, h is determined using Colburn's formula. In case of injection, we use results from a series of tests carried out on a 1/5 scale model of oblique nozzles. The mockup has been fitted with several measurement devices : the mixture function  $\tau$  is measured by colorimetry, in which heat transfer is replaced by mass transfert ; hot water is injected into the branch pipe and the fluid temperature at each point (see figure 4 for the locations)

are measured by thermocouples. For each location, the two following parameters are measured :

$\left(\frac{h}{h_p}\right)$  and  $\tau$  as a function of  $\left(\frac{V_i}{V_p}\right)$  with :

- $\frac{V_i}{V_p}$  : relative injection rate ( $V_i$  : injection fluid rate,  $V_p$  : primary fluid rate),
- $\frac{h}{h_p}$  : heat exchange coefficient rate (h at the sensor level,  $h_p$  for the primary fluid),
- $\tau$  : function of the mixture at the point of measurement (between 0 to 1).

The heat exchange coefficient is deduced from the latter ratio :

$h = \eta \cdot \left(\frac{h}{h_p}\right) \cdot h_p$ , where  $\eta$  is a scale coefficient (1 on our geometry). The fluid temperature at the point of measurement can be determined with the following formula :  $T = T_p + (T_i - T_p) \cdot \tau$ , with :  $T_p$  = main fluid temperature,  $T_i$  = injection fluid temperature.

### 7. Thermal analysis

We first proceed to a 1-D thermal analysis in order to select the eleven transients covering all the other ones according to the criteria : maxima of  $\Delta T_1$  and maxima of  $\Delta T_2$ , for the two areas : branch pipe to lateral nozzle transition, lateral reinforcement.

After the 3-D heat conduction analysis was solved, we selected some instants in the

duration of this conduction associated with the extreme values of the five following critical terms :  $\Delta T1$ ,  $\Delta T2$  (related to the inside or outside skin),  $[T_i - T_m]$  (difference between the inside temperature and the average temperature),  $T_e - T_m$ . Such a selection was undertaken in the weld between the branch line and the connexion and in the connexion reinforcement.

#### 8. Thermoelasticity

The 3-D thermal stress analysis was performed for the sixty instants selected. Both ends of the structure are free and the bottom line of the pipe's symmetry plane is constrained.

#### 9. Procedure for stress indices determination

We selected meridional planes in which there are the extreme values of peak stress intensity range : SP, for both the branch pipe to lateral nozzle transition and the lateral reinforcement. In our case, we keep three planes for the first area (2 in the symmetry plane, one perpendicular to this plane) and two for the reinforcement : acute and obtuse corners of the connection reinforcement. The distribution of peak stress along a linear radial path in each plane was divided into membrane and secondary bending components to obtain the stress indices. For the most conservative thermal shock : depressurization of the main primary circuit (see figure 5), we know SP and some calculations determined the primary plus secondary stress range SN :

$$SN = \frac{E \cdot \alpha}{2(1-\nu)} \cdot |\Delta T1| + C3 \cdot Eab \cdot (\alpha_a \cdot Ta - \alpha_b \cdot Tb) \quad (1)$$

$$SP = \frac{E \cdot \alpha}{2(1-\nu)} \cdot K3 \cdot |\Delta T1| + K3 \cdot C3 \cdot Eab \cdot (\alpha_a \cdot Ta - \alpha_b \cdot Tb) + \frac{E \cdot \alpha}{(1-\nu)} \cdot |\Delta T2| \quad (2)$$

We will perform 1-D thermal analyses using this transient at each linear radial path corresponding to those of the 3-D model associated with the extreme values of SN and SP. The results of this transient heat conduction, with h taken into account at the respective location of the 3-D model, will give us the thermal distribution in terms of :  $\Delta T1$ ,  $\Delta T2$ ,  $|Ta - Tb|$ .

The comparison between the 3-D stresses and 1-D thermal results determines the thermal stress indices :

$$K3 = \frac{SP - \frac{E \cdot \alpha}{1-\nu} \cdot |\Delta T2|}{SN} \quad (3)$$

$$C3 = \frac{SP - \frac{E \cdot \alpha}{1-\nu} \cdot |\Delta T2| - K3 \cdot \frac{E \cdot \alpha}{2(1-\nu)} \cdot |\Delta T1|}{K3 \cdot Eab \cdot (\alpha_a \cdot Ta - \alpha_b \cdot Tb)} \quad (4)$$

#### 10. Preliminary results

##### . Thermal :

(See figures 6 to 9 for the isotherms) : we can appreciate the immediate thermal response of this nozzle after the shock initiation. The conduction in the wall thickness is regular and low, and at the end of the transient the whole nozzle is homogeneous. The precision of these results show us how this refined mesh is adequate for this kind of analysis.

##### . Stresses :

The maximum value of the stress (1000 MPa) occurs at a location on the inside skin just above the largest thickness of the acute corner. The nozzle is quickly highly constrained, ended by an homogeneous low stress state at the end of the shock. (See figures 10 to 13)

11. Conclusion

This study will allow us the thermal stress indices determination C3 (linear stress) and K3 (peak stress) for the 45 degrees lateral connection. These indices will be codified in the RCC-M code and could be used on similar geometry. Later published, they will be compared to those of the literature.

The thermal stresses files in the crotch area could be used in fracture mechanics topic (fatigue propagation and tearing initiation) for postulated flaws.

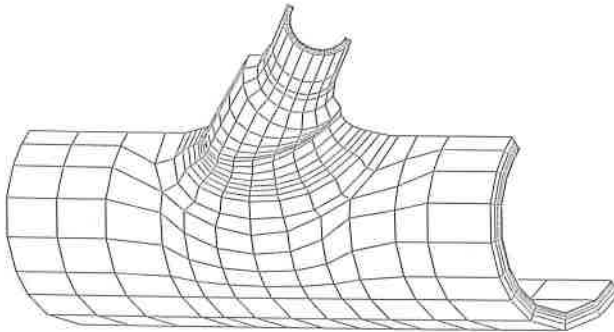


Figure 1 : 3-D Finite Element Mesh

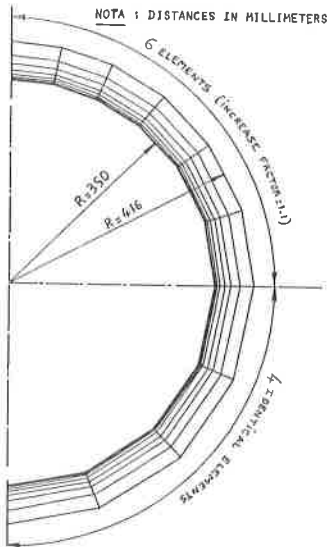


Figure 2 : Element Description in run pipe sections

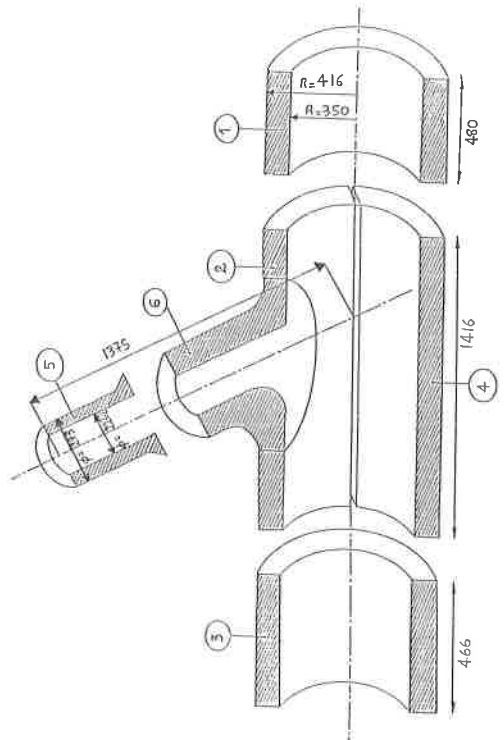


Figure 3 : Breakdown of Structure

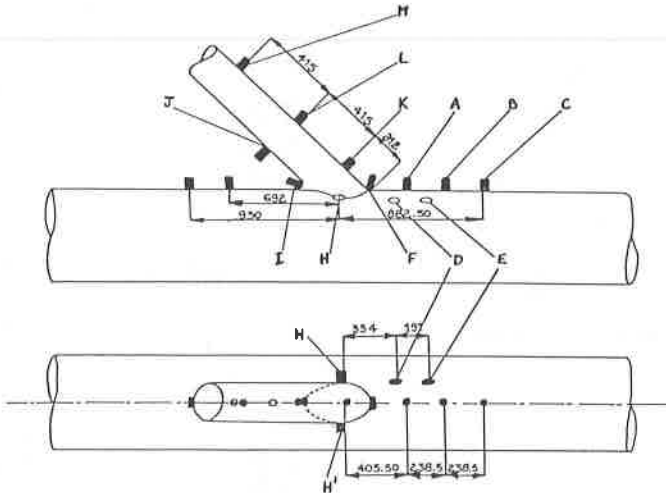


Figure 4 : Sensors location

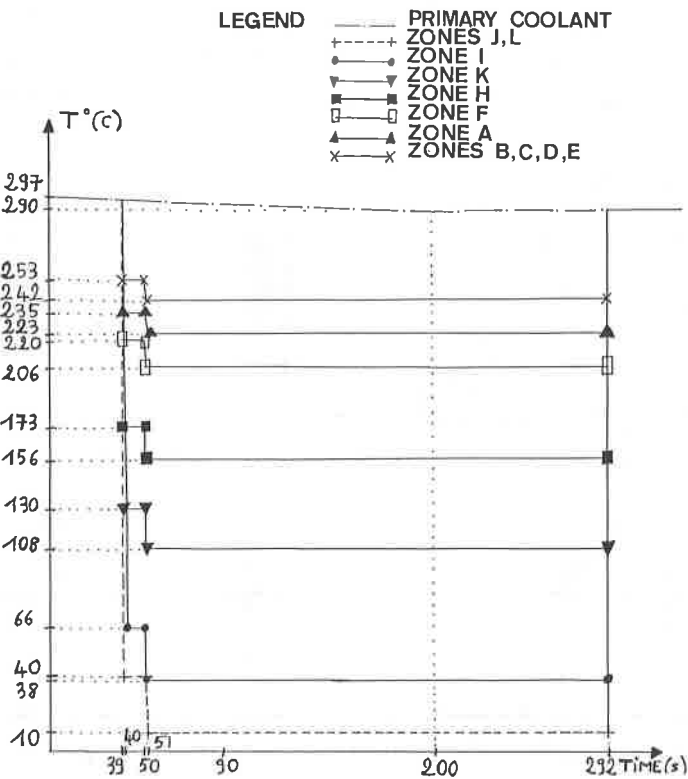


Figure 5 : Inadvertant depressurization of the reactor coolant system

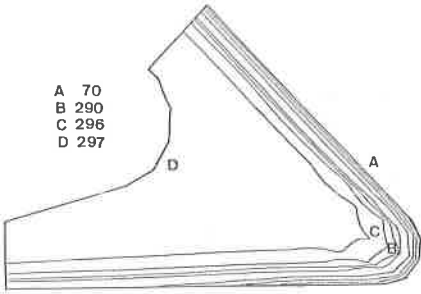


Figure 6 : Isotherms Symetry plane -  
Time 52.5 S

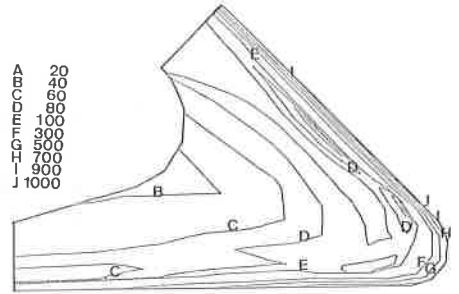


Figure 10 : Isotrescas symetry plane  
Time 52.5 S

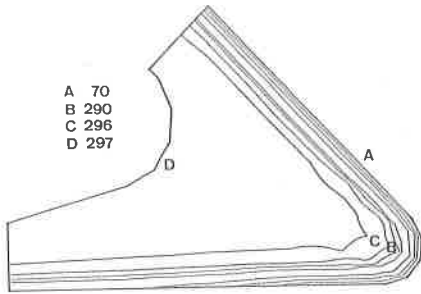


Figure 7 : Time 54 S

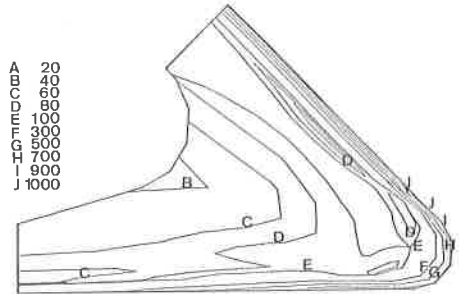


Figure 11 : Time 54 S

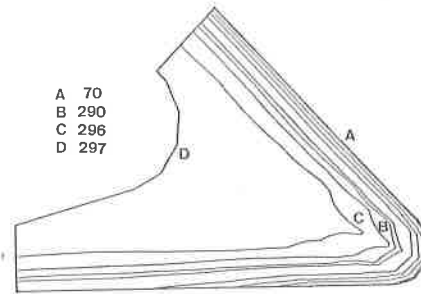


Figure 8 : Time 61.5 S

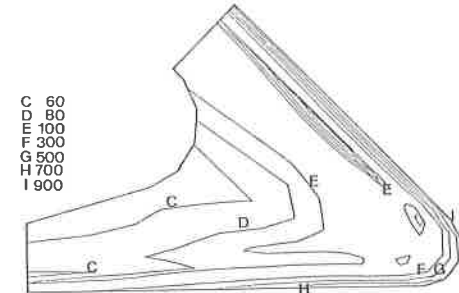


Figure 12 : Time 61.5 S

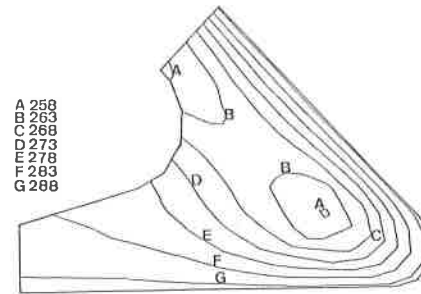


Figure 9 : Time 780 S

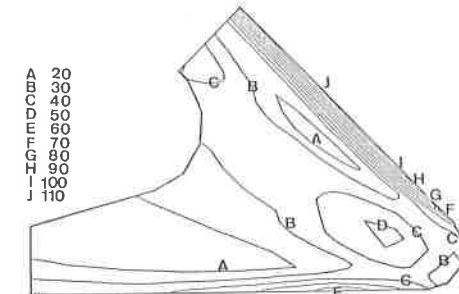


Figure 13 : Time 780 S